

# Development of Vacuum Packaged CMOS Thermoelectric Energy Harvester

Chengkuo Lee<sup>1,2\*</sup>, Member, IEEE and Jin Xie<sup>1</sup>

<sup>1</sup> Institute of Microelectronics (IME), Agency for Science, Technology and Research (A\*STAR), Singapore 117685

<sup>2</sup> Department of Electrical and Computer Engineering, National University of Singapore, Singapore 117576

**Abstract -** A new concept of MEMS based thermoelectric power generator (TPG) is investigated in this study. By using solder based wafer bonding technology, we can bond three pieces of wafers to form vacuum packaged TPG. According to the finite element method and analytical modeling results, the output power per area of device is derived as  $68.6 \mu\text{W}/\text{cm}^2$  for temperature difference of  $6^\circ\text{C}$  between two ends of thermocouple junctions. It shows that the proposed device concept is an effective and low cost approach to enhance the output voltage.

**Keywords:** MEMS, Thermoelectric, Power generator, Energy harvester

## I. INTRODUCTION

Traditionally, electronic devices have relied on batteries as the power sources because they are reliable, easily accessible and convenient to use. However, batteries can only operate over a finite period of time, after which they will have to be changed. Frequent replacement of batteries is not appropriate in few applications such as implantable biomedical devices and wireless sensor networks in harsh environment. Clean energy like solar energy and MEMS (microelectromechanical systems) energy harvesters are promising alternatives. Silicon solar cell of average efficiency can produce about  $15 \text{ mW}/\text{cm}^2$  under direct sunlight, while the same solar cell can only produce about  $10 \mu\text{W}/\text{cm}^2$  in normal office lighting. Advances in low power VLSI design and CMOS (complementary metal oxide semiconductor) fabrication have reduced power requirements for ICs to the point that self-powered wireless sensor network nodes are now feasible. Vibration based MEMS energy harvesters have been investigated for power sources of wireless sensor network applications [1, 2]. MEMS energy harvesters using thermoelectric energy transduction mechanism is a promising power source in the realization of a body area network which consists of a set of wireless sensors and actuators for providing health, sports, comfort, and safety monitoring functions to the users [3]. The thermoelectric method can convert ambient heat flux (thermal energy) into voltage output (electrical energy). In other words, thermoelectric devices convert waste heat from human body into electrical power, i.e., the thermoelectric power generators (TPGs). The n-doped and p-doped polycrystalline silicon are the available thermoelectric materials in CMOS process [4]. With the aids of microelectromechanical systems (MEMS) technology, we can make very thin membrane structure comprising n/p polySi thermocouples by deploying the bulk micromachining to remove the underneath silicon substrate [5,

6]. The appropriate heat flux path is necessary to be managed in order to create the largest temperature difference between two ends of thermocouples, i.e., the hot and cold junctions. The output voltage of TPGs is in proportion to said temperature difference. We proposed a new MEMS TPG configuration in wafer bonding packaged vacuum structure. We introduced a new concept of heat dissipation path (HDP) for enhancing the temperature difference between hot and cold junctions. The focus of this paper is to develop an approach of design and optimization of this vacuum packaged MEMS TPGs.

## II. DEVICE CONFIGURATION AND DESIGN CONSIDERATION

Recently a membrane type MEMS TPG with underneath air cavity encapsulated by wafer bonding process has been reported by T. Huesgen et al. [7]. Besides, the SU-8, a polymer with high thermal resistance, has been deposited on the top surface of TPG to block the heat loss and to confine the thermocouples as the main heat path, while an additional overcoat of gold film on SU-8 is made to guiding the heat flowing toward the main heat path. We propose a new MEMS TPG design to improve the output voltage by using solder based wafer bonding technology [8] to form sealed vacuum cavities on both sides of MEMS TPG, as shown in Fig. 1. A bottom silicon wafer is bonded to MEMS TPG wafer with backside opening in vacuum chamber.

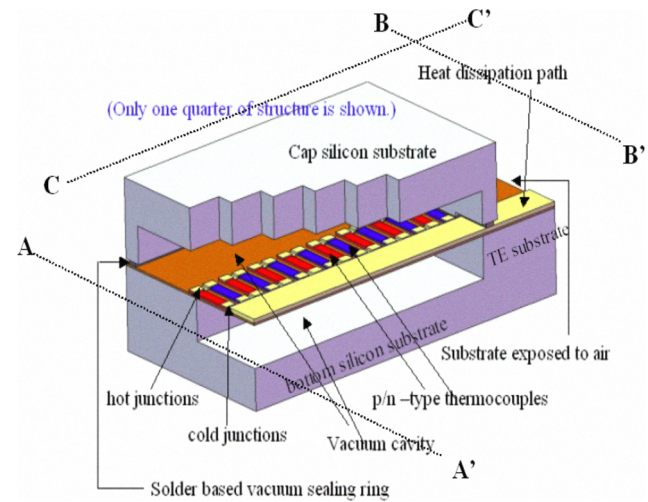


Fig 1. Schematic view of the MEMS TPG with two vacuum cavities formed by wafer bonding (only one quarter of structure is shown.).

This project was partially supported by grants from a joint-funded research project based on University Research Fund R-263-000-475-112 of the National University of Singapore and from the IME, A\*STAR, Singapore.

\*Contact author: [eelc@nus.edu.sg](mailto:eelc@nus.edu.sg); [leek@ime.a-star.edu.sg](mailto:leek@ime.a-star.edu.sg)

Thus the underneath cavity is sealed in vacuum. A cap wafer with cavities is further bonded to the top surface of MEMS TPG wafer such that a top vacuum cavity is formed, as shown in Fig. 2 (a). To illustrate our concept, the cross-section views of proposed MEMS TPG along A-A', B-B' and C-C' lines have been depicted in Fig. 2 (a), (b) and (c), respectively. The bottom Si substrate can be attached on the human skin or any other hot objects available, while the peripheral surface of Si thermoelectric substrate is exposed to ambient air of 25°C, as depicted in Fig.2 (b) and (c).

by vacuum cavities, respectively. There are 64 thermocouples on the thermoelectric structure area. Because it is a symmetric structure, we only built one quarter of structure in the FEA model as shown in Fig. 3 (a) to (c), while we did not create the cap structure in these FEA models and we assumed the top surface of device is either in air or in vacuum. The width, length and thickness of thermocouple strip are  $6\mu\text{m}$ ,  $30\mu\text{m}$  and  $1\mu\text{m}$ , respectively. In current study, we also introduce a new concept of heat dissipation path for enlarging the temperature difference between the cold and hot junctions as shown in Fig. 2 (a), (b), and (c), and Fig. 3 (c).

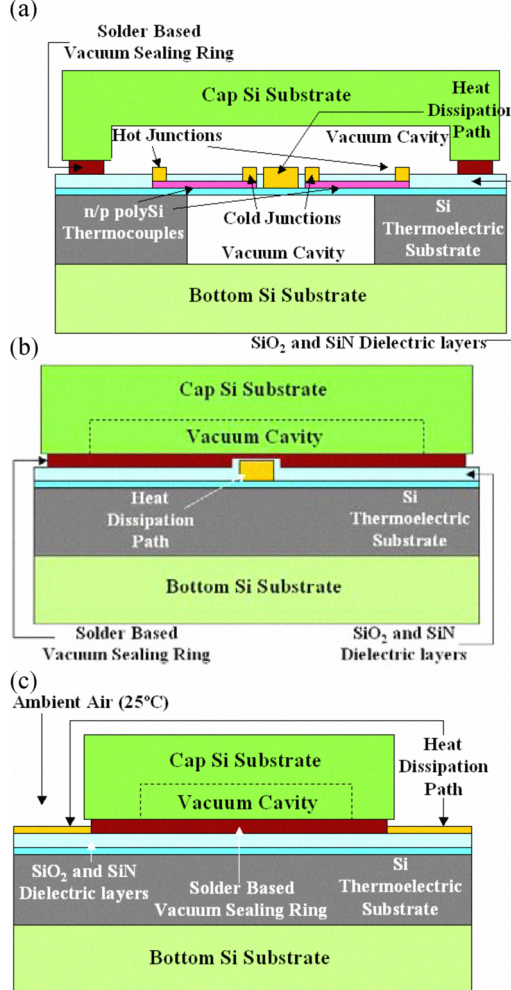


**Fig. 2.** The schematic drawings of cross-sectional views of MEMS TPG in Fig. 1, (a) TPG view along thermocouple strips (A-A' line); (b) TPG view along edge of chip (B-B' line) where the heat dissipation path is exposed to air; (c) TPG view along longitudinal direction of heat dissipation path (C-C' line), when we look at the sidewall of three bonded chips.

We deploy finite element analysis (FEA) approach to simulate the temperature distribution based on ANSYS software. Fig. 3 (a), (b) and (c) display the temperature contour plots for thermoelectric structure on Si substrate in air ambient, a thermoelectric suspended membrane surrounded by ambient air, and a thermoelectric suspended membrane encompassed

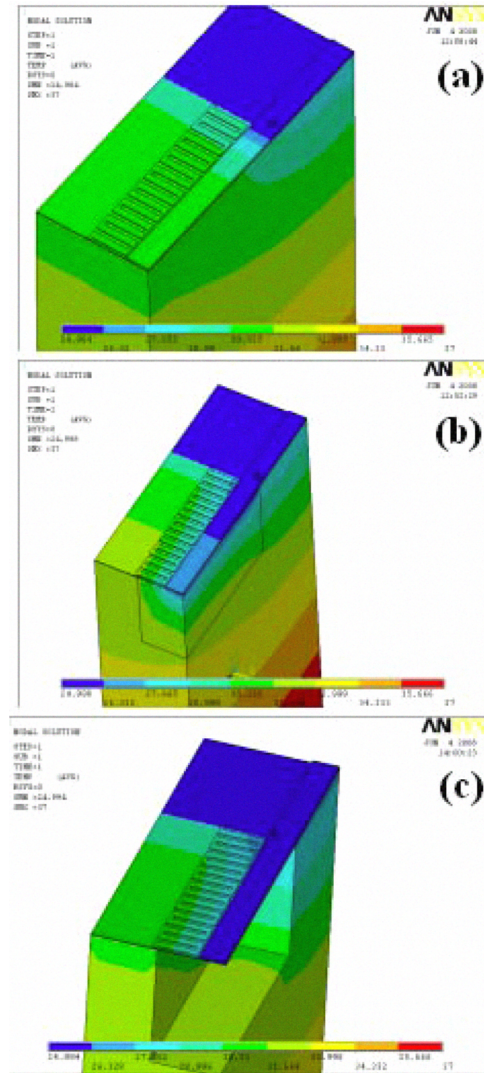


Fig.3: The temperature contour plots of MEMS TPG, (a) the TPG on Si substrate without underneath vacuum cavity and its surface exposed to air, (b) the TPG on Si substrate with underneath air-filled cavity and its surface exposed to air, (c) the TPG packaged in vacuum as same as the configuration shown in Fig.1, where the ambient air is maintained as 25°C, the bottom surface of bottom Si substrate is kept as 37°C, and the depth of vacuum cavity is 100μm.

This heat dissipation path of  $30\mu\text{m}$  in width and  $2\mu\text{m}$  in thickness is made of Al metal film and is arranged along the cold junctions of thermocouples. It should be noticed that only  $15\mu\text{m}$  wide heat dissipation path has been made in the quarter structure in FEA models. This simple and unique structure can effectively transfer the heat from cold junctions of thermocouples to the peripheral substrate surface where it is exposed in ambient air (Fig. 3 (c)). Fig. 3 (a) shows that the temperature difference between hot and cold junctions is very small for the thermoelectric structure without underneath air cavity. When an air cavity is created underneath the suspended thermoelectric structure, as shown in Fig. 3 (b), the heat flux path is changed and the increased temperature difference is observed as well. However, significant heat conduction and convection still happen in the heat flux path from the suspended thermoelectric structure to ambient air. As further improvement, the suspended thermoelectric structure is packaged in wafer-bonded vacuum package, as shown in Fig. 3 (c). The vacuum package can effectively increase the temperature difference through elimination of heat conduction and convection in air cavity.

In order to identify the temperature distribution of different thermocouple strips among the 16 strips, we define each strip as the thermal leg from the position 1 (the closest one to the edge of membrane next to the peripheral substrate) to position 16 (the one at the center of membrane). The temperature difference is maintained at about  $6^\circ\text{C}$  from the thermal leg 4 to the center (Fig. 4 (a)). In contrast to the results shown in Fig. 3 (c) and Fig. 4 (a), almost no temperature difference and average temperature difference of  $3\text{--}4^\circ\text{C}$  are observed in Fig. 3 (a) and (b), respectively. Secondly we derived the temperature difference depending on various depth of underneath vacuum cavity of  $100\mu\text{m}$ ,  $70\mu\text{m}$ ,  $50\mu\text{m}$  and  $20\mu\text{m}$ , respectively, as shown in Fig. 4 (b). The maximum temperature difference is decreased for  $1^\circ\text{C}$  when we compare the curve of  $100\mu\text{m}$  with the one of  $50\mu\text{m}$ . Thus we maintain the vacuum depth of  $100\mu\text{m}$  in all analytical simulation in next section.

### III. ANALYTICAL MODELING OF TPG OUTPUT POWER

In the second part of simulation, we conduct the TPG output power optimization with respect to various widths of heat dissipation path in order to clarify the influence of heat dissipation path to the output power. First of all, we review the background physics as next. The equation 1 shows that the open circuit voltage  $U_o$  generated by a TPG is proportional to the number of thermocouples  $m$ , the relative Seebeck coefficient  $\alpha$  of the used thermocouple materials and the temperature difference  $\Delta T_G$  between cold and hot junctions. We use  $160\mu\text{V/K}$  [4] as the average Seebeck coefficient in the analytical simulation.

$$U_o = m\alpha\Delta T_G \quad (1)$$

The maximum output power  $P_o$  can be achieved under

matched load condition, i.e. the load resistance connected to the generator  $R_L$  equals the internal electrical resistance of the generator  $R_G$ :

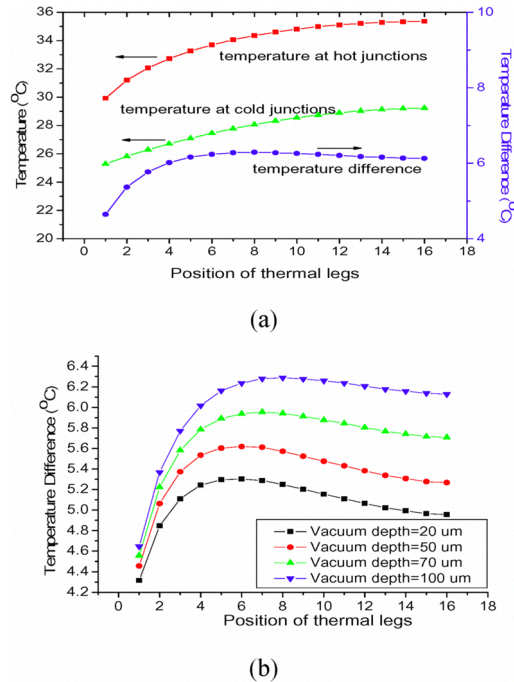


Fig.4: (a) Temperature distribution and the difference versus the various position of thermal legs for the MEMS TPG device as in Fig. 3 (c) where the vacuum depth is  $100\mu\text{m}$ ; (b) Temperature difference versus the various position of thermal legs in case of different depth of vacuum cavity.

$$P_o = UI = \frac{U_o^2}{4R_G} = \frac{m^2\alpha^2}{4R_G} \Delta T_G^2 \quad (2)$$

where  $U$  is the output voltage under load and  $I$  is the electrical current. Assuming that the generator is connected to a cold reservoir and a hot reservoir via the thermal contact resistances  $K_C$  and  $K_H$ , respectively, the temperature drop across the generator  $\Delta T_G$  is expressed as eq. (3), where  $K_G$  is the generators internal thermal resistance and  $\Delta T$  is the temperature difference between hot and cold reservoirs.

$$\Delta T_G = \frac{K_G}{K_G + K_C + K_H} \Delta T \quad (3)$$

For single thermal leg, the thermal resistance  $k$  and electrical resistance  $R$  are derived as eq. (4) and (5), where the  $\lambda$  is thermal conductivity and  $\rho$  is electrical resistivity, respectively.

$$k = \frac{l}{\lambda w t} \quad (4)$$

**Table 1. Optimization of heat dissipation path (HDP) with different width**

Optimized items	Width of HDP ( $\mu\text{m}$ )		
	10	20	30
Output power per area of device ( $\mu\text{W}/\text{cm}^2$ )	54.2	68.6	60.5
Output power per area of thermocouples ( $\mu\text{W}/\text{cm}^2$ )	246.7	309.3	206.4
Length of thermal leg ( $\mu\text{m}$ )	22	18	20
Width of thermal leg ( $\mu\text{m}$ )	10	10	8

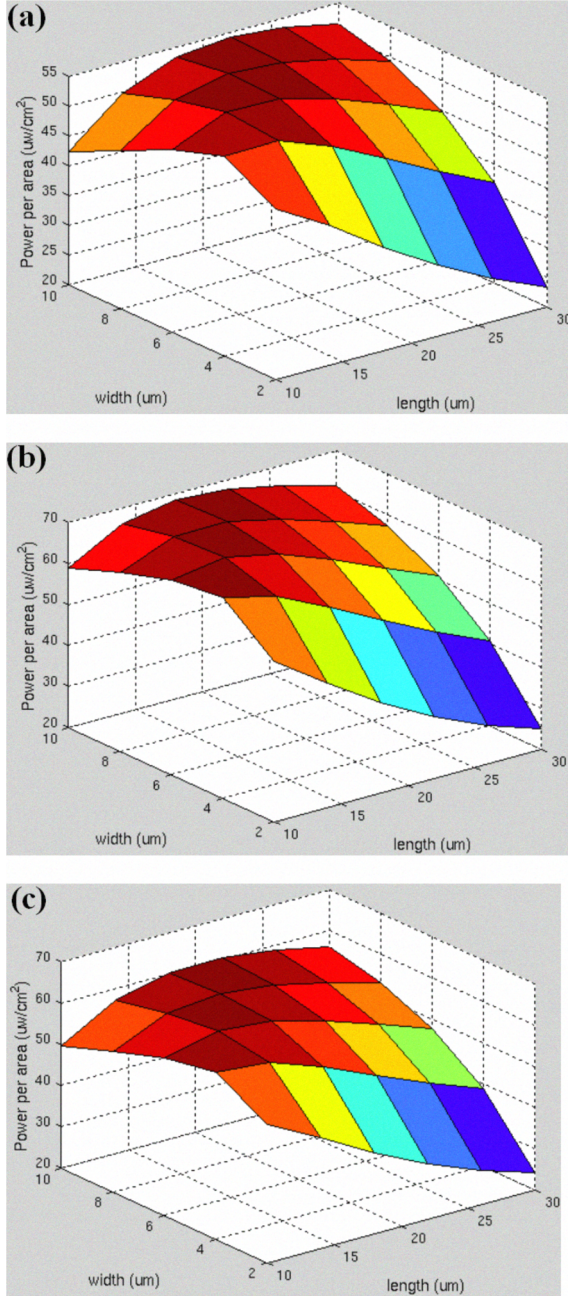


Fig. 5. The optimized output power of TPGs with respect to various cases of different HDP width, (a) HDP of 10  $\mu\text{m}$ ; (b) HDP of 20  $\mu\text{m}$ ; (c) HDP of 30  $\mu\text{m}$ .

$$R = \rho \frac{l}{wt} \quad (5)$$

According to the approach discussed in section 2, we can derive the  $\Delta T$  for various cases in terms of different thermal leg widths and lengths, and width of heat dissipation path (HDP). Fig. 5 (a), (b) and (c) show the derived results in the three cases of heat dissipation path of 10  $\mu\text{m}$ , 20  $\mu\text{m}$ , and 30  $\mu\text{m}$ , respectively. The derived maximum output powers in these three cases are summarized in table 1. Since the effect of width and length of thermal leg on thermal resistance and electrical resistance are contradictory. Thus there is an optimized combination of width and length in each case of different heat dissipation path (HDP). The observed maximum output power per area of device is 68.6  $\mu\text{W}/\text{cm}^2$  in the case of HDP of 20  $\mu\text{m}$ . On the other hand, we can consider another index which is output power per area of thermocouples, when we exclude the area occupied by HDP. Interestingly device of HDP of 20  $\mu\text{m}$  still shows the highest output power as of 309.3  $\mu\text{W}/\text{cm}^2$ . Besides, device with HDP of 10  $\mu\text{m}$  shows the 2nd highest output power as of 246.7  $\mu\text{W}/\text{cm}^2$  than the output power of device with HDP of 30  $\mu\text{m}$ .

#### IV. CONCLUSION

We investigated a new concept of CMOS MEMS based thermoelectric power generators with wafer-bonded vacuum cavities on both side of suspended thermoelectric membrane. The calculated output power per area of device is 68.6  $\mu\text{W}/\text{cm}^2$  at initial temperature difference of 12°C in which the induced temperature difference between two ends of thermocouple junctions is derived as 6°C. This new concept is concluded as an effective approach to enhance the output power.

#### ACKNOWLEDGEMENT

Authors acknowledges A\*STAR HOME 2015 National Research Programme (SERC grant number: 0621150043) for the funding of this project and in-kind contribution from Institute of Microelectronics, A\*STAR. Chengkuo Lee would like to thank the support from grant of Faculty Research Fund R-263-000-358-112/133 for relative activities at the National University of Singapore.

#### REFERENCES

- [1] S. Roundy, P. K. Wright and J. Rabaey, "A study of low level vibrations as a power source for wireless sensor nodes," *Computer Commun.*, Vol. 26, pp.1131-1144, 2003.
- [2] P. D. Mitcheson, E.M. Yeatman, G. K. Rao, A. S. Holmes, T. C. Green,

- "Energy Harvesting From Human and Machine Motion for Wireless Electronic Devices," Proceedings of the IEEE, 96, 1457 (2008).
- [3] T. VonBuren T, P.D. Mitcheson, T.C. Green, E.M. Yeatman, A.S. Holmes, and G. Troster, "Optimization of inertial micropower generators for human walking motion," IEEE Sensors J. Vol. 6, No. 1, pp. 28–38, 2006.
- [4] M. Strasser, R. Aigner, M. Fransch and G. Wachutka, "Miniaturized thermoelectric generators based on poly-Si and poly-SiGe surface micromachining," Sensors and Actuators A, Vol. 97-98, pp.535-542, 2002.
- [5] A. Graf, M. Arndt, M. Sauer and G. Gerlach, "Review of micromachined thermopiles for infrared detection," Meas. Sci. Technol., 18, R59 (2007).
- [6] C.-H. Du and C. Lee, Jpn. "Characterization of Thermopile Based on Complementary Metal-Oxide-Semiconductor (CMOS) Materials and Post CMOS Micromachining," J. Appl. Phys., Part 1, 41, 4340 (2002).
- [7] T. Huesgen, P. Woias, N. Kockmann, "Design and fabrication of MEMS thermoelectric generators with high temperature efficiency," Sensors and Actuators A, doi:10.1016/j.sna.2007.11.032, 2008.
- [8] Y. C. Lee, B. A. Parviz, J. A. Chiou, S. Chen, "Packaging for microelectromechanical and nanoelectromechanical Systems," IEEE Trans. Adv. Packaging, Vol. 26, No. 3, pp. 217-226, Aug. 2003.